Crossflow Topology of Vortical Flows

Miguel R. Visbal* and Raymond E. Gordnier*
Wright Laboratory,
Wright-Patterson Air Force Base, Ohio 45433

Introduction

FLOWS past delta wings and slender bodies of revolution at angle of attack are of obvious importance in aerodynamics. These flows are characterized by the formation of streamwise vortical structures on the leeside of the body. In experimental as well as computational studies, the vortical flow structure is often examined on transverse planes normal to the body axis. On such planes, the projected or sectional streamline pattern typically exhibits crossflow separation.[1] The purpose of this Note is to demonstrate using critical-point theory and computational results for delta wing flows[2,3] that a number of distinct topologies of crossflow separation are possible. In addition, the present results confirm and extend recent experimental findings[4,5] for the instantaneous crossflow topology on pitching delta wings.

Critical-Point Theory

The interpretation of two-dimensional sectional streamline patterns is aided considerably by the use of critical-point theory or phase-space analysis as described for instance by Perry and Chong[6] (and references therein). At critical (or singular) points of the flow, the velocity is zero and the streamline slope is indeterminate. If (u_1, u_2) denote the components of the three-dimensional velocity field projected on a given plane (x_1, x_2), the classification of two-dimensional critical points on this plane is obtained from the divergence $\Delta = \partial u_1/\partial x_1 + \partial u_2/\partial x_2$ and the Jacobian $J = (\partial u_1/\partial x_1)(\partial u_2/\partial x_2) - (\partial u_1/\partial x_2)(\partial u_2/\partial x_1)$, as shown in Fig. 1a. The different types of critical points are saddles, nodes, and foci. The foci and nodes can be either stable (attracting) or unstable (repelling), depending on the sign of Δ.

Another important but less recognized feature encountered in the topology of sectional streamline patterns is the closed "bifurcation line" or "limit cycle."[6] A limit cycle is a closed isolated trajectory to which other nonclosed trajectories asymptote (stable limit cycle) or emanate from (unstable limit cycle). A schematic of a stable limit cycle is given in Fig. 1b. An unstable limit cycle may be obtained from this figure by reversing the direction of the arrows. If a limit cycle exists in the sectional streamline pattern, it must enclose at least one critical point that cannot be a saddle. Furthermore, the divergence of the projected velocity field on the plane must change sign in the region where the limit cycle exists.

Results and Discussion

To show the application of critical-point theory to crossflow separation, two examples taken from computed flowfields about delta wings are considered. The first case pertains to the structure of transient vortex breakdown above a pitching delta wing computed in Ref. 2 and studied experimentally by Magness et al.[4] and Lin and Rockwell.[7] Calculations were performed for a 75-deg sweep delta wing subject to a ramp-type pitch maneuver from 25- to 50-deg angle of attack. Details of the computational procedure, grid sensitivity study, and favorable comparison with the experimental data are provided in Ref. 2.

Received May 11, 1993; revision received Oct. 27, 1993; accepted for publication Nov. 1, 1993.

*Aerospace Engineer, CFD Research Branch, Aeromechanics Division. Senior Member AIAA.

The computed instantaneous crossflow topology at several streamwise stations along the wing is shown in Fig. 2 at a nondimensional time $tU_\infty/C = 0.4$ after the wing has completed its pitching motion. The corresponding distribution of the streamwise velocity component along the leading-edge vortex axis is given in Fig. 3. (For convenience, the vortex axis is arbitrarily defined as a straight line emanating from the apex and passing through the point of minimum total pressure in the vortex core on a plane sufficiently upstream of breakdown.) It can be seen that vortex breakdown (defined in terms of $u = 0$) occurs just downstream of the 60% chord location. Near the apex ($X/C = 0.13$), the crossflow topology of the primary vortex is characterized by the usually assumed stable (spiraling in) focus (Fig. 2a). At $X/C = 0.34$ (Fig. 2b), the sectional streamlines emanating from the leading edge spiral inward, but the streamlines in the core spiral outward, with a stable limit cycle (Fig. 1b) between the two regions. At the location $X/C = 0.6$ (Fig. 2c), the topology is characterized by an unstable (spiraling out) focus as first shown by Magness et al.[4] Finally, at $X/C = 0.9$ (Fig. 2d), downstream of breakdown, the flow in the core begins to spiral inward, whereas away from the axis the flow spirals outward, and an unstable limit cycle appears. It should also be noted that in Figs. 2a and 2b the sectional streamline emanating from the wing leading edge is entrained into the vortical flow, unlike Figs. 2c and 2d in which no entrainment is observed. The calculations reveal that the crossflow topology of the primary vortex can be characterized by either a stable or an unstable focus and that the transformation between the two topologies takes place through the appearance of limit cycles. The existence of limit cycles has also been previously observed on a plane that cuts a multicelled vortical structure.[6] However, the limit cycle of Fig. 2b, which occurs upstream of vortex breakdown, is not associated with reverse axial flow in the vortex core but rather with the axial deceleration and radial divergence of the flow, as explained next.

The type of two-dimensional critical point in a crossflow (X = const) plane associated with the primary vortex is determined (see Fig. 1a) by the divergence $\Delta = v_Y + w_Z$ and the Jacobian $J = v_Y w_Z - v_Z w_Y$ of the projected velocity field at the critical point. If $J > \Delta^2/4$, the critical point is a focus, either stable for $\Delta < 0$ or unstable for $\Delta > 0$. For the pattern of Fig. 2b, $J/(U_\infty/C)^2 = 2.5 \times 10^4$ and $\Delta/(U_\infty/C) = 4.5$, and therefore the focus must be unstable. Since the outer flow is spiraling inward, a limit cycle exists and lies in a region where Δ changes sign. If the flow is assumed to be effectively incompressible, Δ can be approximated by $-\partial u/\partial X$ using the equation of mass conservation. Therefore, the patterns of Fig. 2 may be approximately correlated with the corresponding streamwise velocity distribution along the core given in Fig. 3. For $X/C = 0.13$ and 0.9 (Figs. 2a and 2d), $\partial u/\partial X > 0$ (vortex stretching), and the sectional streamlines exhibit a stable focus. On the other hand, for $X/C = 0.34$ and 0.6, an unstable focus is present due to the negative streamwise velocity gradient (vortex compression). Since sectional streamline patterns are not necessarily invariant with the orientation of the plane,[1] the crossflow topology was re-examined on transverse planes normal to the vortex axis but was found to be essentially the same. Therefore, the various topologies of Fig. 2 are not due to the angle of the plane relative to the vortex axis (as could be the case) but rather to stretching and compression of the vortex core.

The preceding straightforward application of critical-point theory to the interpretation of sectional streamline patterns also suggests that the various crossflow topologies observed are not restricted to the case of unsteady vortex breakdown. To show this, the next example considered is the steady flow past a 80-deg sweep delta wing at an angle of attack of 30 deg. Details of the computations and comparison with experiments are given in Ref. 3. The crossflow topology at the 60% chord location is shown in Fig. 4. The topology of the primary vortex is found to be characterized by an unstable focus and

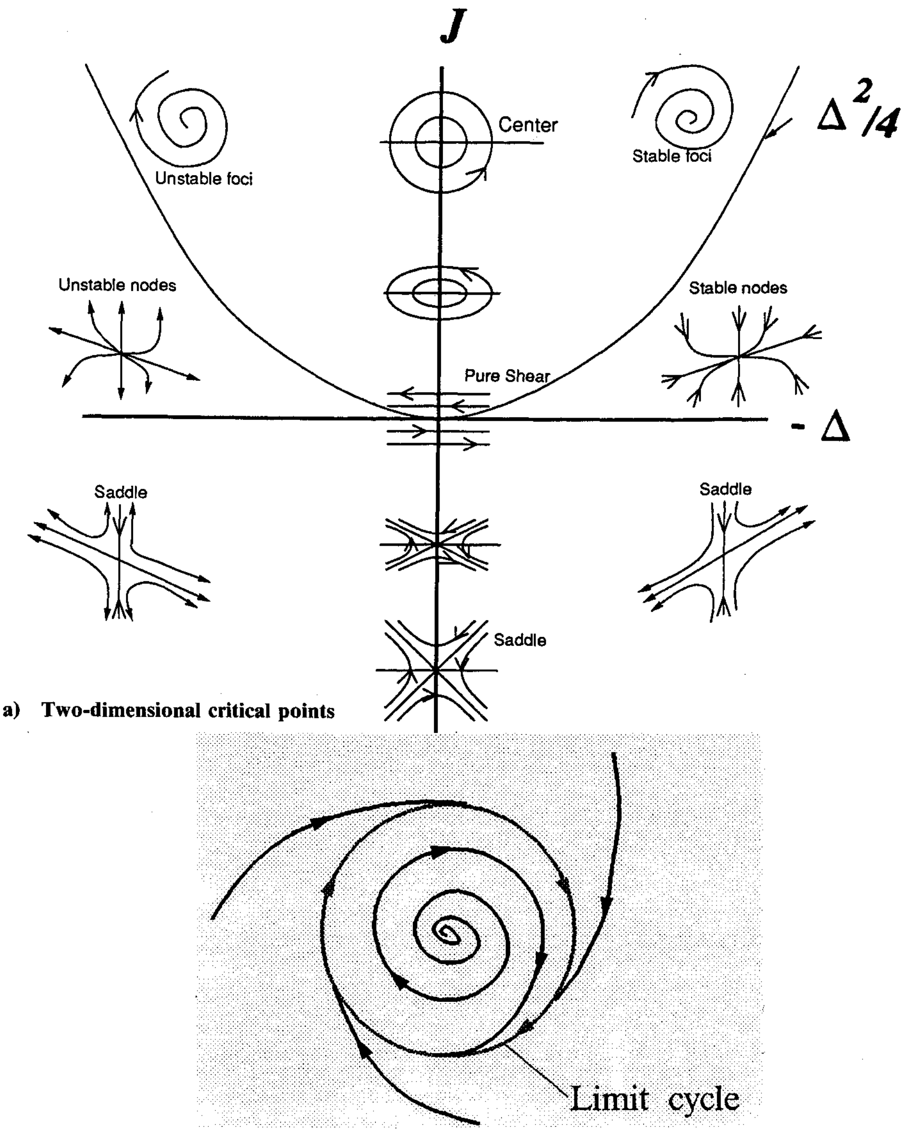

a) **Two-dimensional critical points**

b) **Stable limit cycle**

Fig. 1 Critical-point concepts.

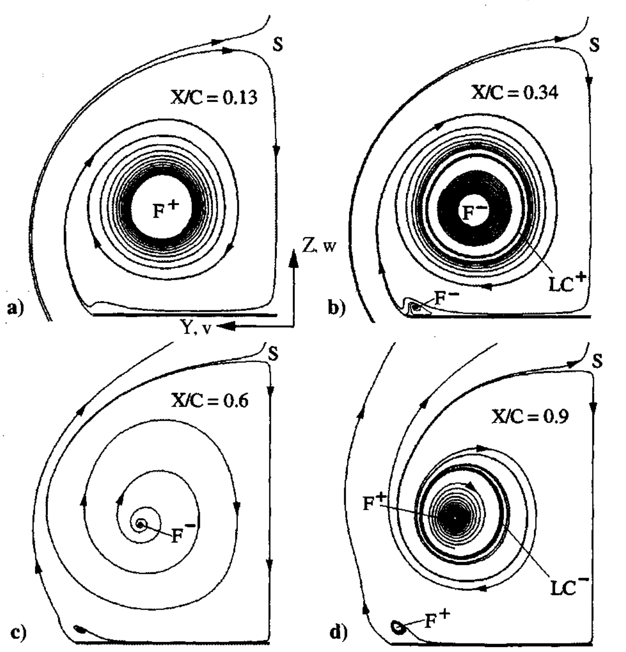

Fig. 2 Instantaneous crossflow topology at select chordwise stations above a 75-deg sweep delta wing (F^+ and F^-: stable and unstable focus; LC^+ and LC^-: stable and unstable limit cycle; S: saddle).

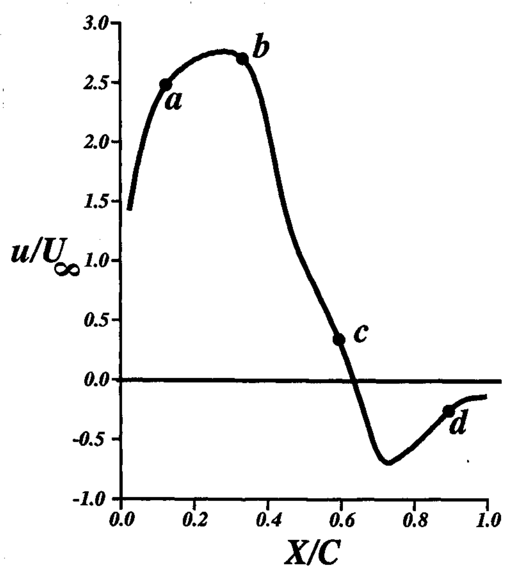

Fig. 3 Streamwise velocity distribution along vortex core (points *a*, *b*, *c*, and *d* correspond to the streamwise stations of Fig. 2).

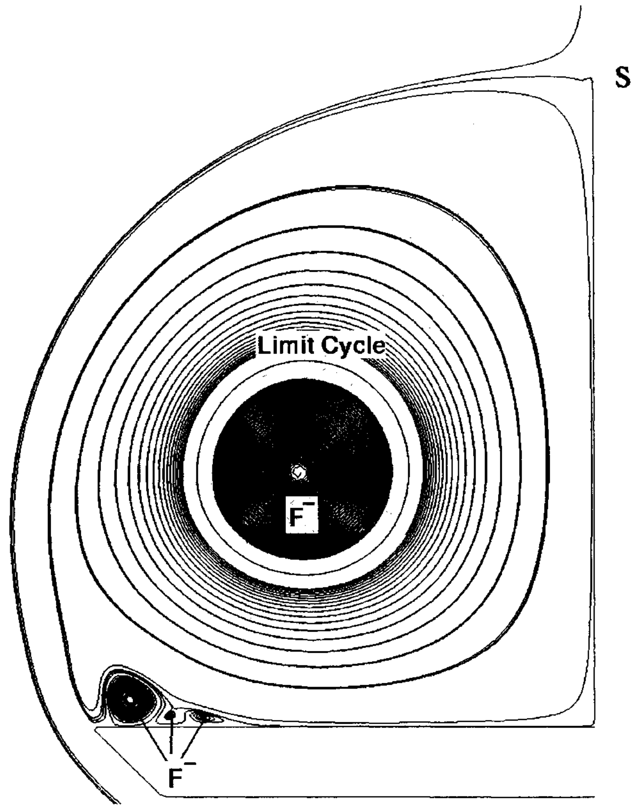

Fig. 4 Crossflow topology at the 60% chord location above an 80-deg sweep delta wing at 30-deg angle of attack.

limit cycle and not by the stable focus commonly assumed. Examination of the flow also shows that the unstable focus corresponds to a negative value of $\partial u/\partial X$.

Although the preceding discussion has been restricted to the primary vortex, different crossflow topologies are also possible for the secondary vortical structures. For instance, in Fig. 2b, the secondary vortical structure near the wing displays an unstable focus, whereas in Fig. 2d, a stable focus is observed. Also, in Fig. 4, the secondary structures show several unstable foci. Finally, unstable foci and limit cycles are also found (but not included here) in the topology of the vorticity vector field projected on a crossflow plane.

The present computational results and the application of critical-point theory clearly show that the usually assumed flow pattern of crossflow separation, characterized by a stable focus, is not universally valid. The crossflow topology of vortical flows may also display unstable foci and limit cycles. The specific type of topology can be correlated with the stretching and compression along the vortex core. The preceding examples of crossflow separation indicate that care should be exercised in the interpretation of both computational and experimental results of vortical flows past wings and forebodies at high angles of attack.

References

[1]Chapman, G. T., and Yates, L. A., "Topology of Flow Separation on Three-Dimensional Bodies," *Applied Mechanics Reviews*, Vol. 44, No. 7, 1991, pp. 329–345.

[2]Visbal, M. R., "Structure of Vortex Breakdown on a Pitching Delta Wing," AIAA Paper 93-0434, Jan. 1993.

[3]Gordnier, R., and Visbal, M., "Numerical Simulation of Delta-Wing Roll," AIAA Paper 93-0554, Jan. 1993.

[4]Magness, C., Robinson, O., and Rockwell, D., "Instantaneous Topology of the Unsteady Leading-Edge Vortex at High Angle of Attack," *AIAA Journal*, Vol. 31, No. 8, 1993, pp. 1384–1391.

[5]Hoang, N. T., Rediniotis, O. K., and Telionis, D. P., "3-D LDV Measurements Over a Delta Wing in Pitch-Up Motion," AIAA Paper 93-0185, Jan. 1993.

[6]Perry, A., and Chong, M., "A Description of Eddying Motions and Flow Patterns using Critical-Point Concepts," *Annual Review of Fluid Mechanics*, Vol. 19, 1987, pp. 125–155.

[7]Lin, J.-C., and Rockwell, D., "Transient Structure of Vortex Breakdown on a Delta Wing at High Angle of Attack," manuscript in preparation, 1994.

Asymptotic Behavior of Solutions of the Renormalization Group K-ϵ Turbulence Model

A. Yakhot,* I. Staroselsky,† and S. A. Orszag‡
Cambridge Hydrodynamics, Inc.,
Princeton, New Jersey 08542

Introduction

At the present time, the only efficient way to calculate turbulent flows in complex geometries of engineering interest is to use Reynolds-averaged Navier-Stokes (RANS) equations. As compared to the original Navier-Stokes problem, these RANS equations possess much more complicated nonlinear structure and may exhibit far more complex nonlinear behavior. In certain cases, the asymptotic behavior of such models can be studied analytically which, aside from being an interesting fundamental problem, is important for better understanding of the internal structure of the models as well as to improve their performance.

Governing Equations and Analysis

In this work, we analyze the renormalization group (RNG) K-ϵ turbulence model, derived directly from the incompressible Navier-Stokes equations.[1,2] It has already been used to calculate a variety of turbulent and transitional flows in complex geometries.[3] In high-Reynolds-number flow regions, the dynamical transport equations for mean turbulent kinetic energy K and mean dissipation rate ϵ are

$$\frac{\partial K}{\partial t} + U_j\frac{\partial K}{\partial x_j} = \nu_T S^2 - \epsilon + \frac{\partial}{\partial x_j}\left(\alpha\nu\frac{\partial K}{\partial x_j}\right) \tag{1}$$

$$\frac{\partial \epsilon}{\partial t} + U_j\frac{\partial \epsilon}{\partial x_j} = \frac{\epsilon}{K}C_{\epsilon 1}\nu_T S^2 - C_{\epsilon 2}\frac{\epsilon^2}{K} - \frac{\nu_T S^3(1-\eta/\eta_0)}{1+\beta\eta^3} + \frac{\partial}{\partial x_j}\left(\alpha\nu\frac{\partial \epsilon}{\partial x_j}\right) \tag{2}$$

Here U_j is the mean velocity, α is the inverse turbulent Prandtl number, $\nu = \nu_T + \nu_0$ is the total viscosity, ν_T is the turbulent viscosity, $S = (2S_{ij}^2)^{1/2}$, $S_{ij} = 1/2(\partial U_i/\partial x_j + \partial U_j/\partial x_i)$ is the mean strain rate, and η is the dimensionless strain-rate parameter $\eta = KS/\epsilon$. The effective eddy viscosity ν and turbulent Prandtl number α are obtained using the RNG scale elimination procedure which yields their functional dependence on the dynamic variables K and ϵ. In the high-Reynolds-number regions of the flow, the asymptotic values of ν and α are $\nu \approx \nu_T = C_\mu K^2/\epsilon$ and $\alpha = 1.39$, and the values of other quantities appearing in Eqs. (1) and (2) are $C_{\epsilon 1} = 1.42$, $C_{\epsilon 2} = 1.68$, $\beta = 0.012$, $\eta_0 = 4.38$, and $C_\mu = 0.084$.

In the near-wall (low-Reynolds-number) regions of wall-bounded turbulent flows, the turbulent viscosity turns off ($\nu_T = 0$)

Received June 2, 1993; revision received Aug. 31, 1993; accepted for publication Sept. 1, 1993.

*Senior Scientist, P. O. Box 1403; also Department of Mechanical Engineering, Ben-Gurion University of the Negev, Beersheva 84105, Israel.

†Senior Scientist, P. O. Box 1403.

‡Professor, P. O. Box 1403; also Applied and Computational Mathematics, Princeton University, Princeton, NJ 08544.